MultiCraft

International Journal of Engineering, Science and Technology
Vol. 3, No. 5, 2011, pp. 1-19

INTERNATIONAL JOURNAL OF ENGINEERING, SCIENCE AND TECHNOLOGY

www.ijest-ng.com

Experimental study of wind-induced pressures on buildings of various geometries

J.A. Amin[1]*, A.K. Ahuja[2]

[1*]*Department of Civil Engineering, Sardar Vallbhbhai Patel Institute of Technology, Vasad, INDIA*
[2] *Department of Civil Engineering, Indian Institute of Technology Roorkee, INDIA*
[*]*Corresponding Author: e-mail: jamin_svit@yahoo.com, Tel +91-2692-274766, Fax. +91-2692-274540*

Abstract

This paper presents the experimental investigation of wind pressure distributions on models of typical plan shape buildings over an extended range of wind incidence angles of 0° to 180° at an interval of 15°. Two L-shaped and two T-shaped models of same plan area and height but having the different dimensions were tested in a closed circuit wind tunnel under boundary layer flow. The models were made from Perspex sheets at a geometrical scale of 1:300. Fluctuating values of wind pressures are measured at pressure points on all the sides of the models and mean, maximum, minimum and r.m.s. values of pressure coefficients were evaluated from pressure records. It is observed that plan shape and dimensions of models significantly affects the wind pressure distributions on different faces of the models. The location and magnitude of the measured peak pressure coefficient vary considerably with wind direction. The influence of shifting the upstream block from edge of the downstream block to center of it, which transforms the L-shape into T-shape model, is also noticeable on the pressure coefficient distribution.

Keywords: Wind pressure coefficients; L-shape and T-shape models; Wind tunnel testing; Wind incidence angle.

1. Introduction

Wind pressures on buildings are influenced by the building geometry, angle of wind incidence, surroundings and wind flow characteristics. There are many situations where available database, codes/standards and analytical methods cannot be used to estimates the wind pressure coefficients and wind loads on the claddings and supporting system of buildings, for example, the aerodynamic shape of the building is uncommon/complex. However in such situations, more accurate estimation of wind pressure coefficients on the building claddings are obtained through model test in boundary layer wind tunnel (Suresh Kumar et al., 2006). Further the pressure coefficients/loads from standards are meant to be upper bound scenario covering almost all cases and having following limitations. Wind load/pressure information (i) does not account the aerodynamic effect of the actual shape of the structure since they are based on box like buildings and (ii) do not allow for any detailed directional effects and assume that the design wind speed will always occur from the aerodynamically severe wind direction. On the other hand, wind tunnel model studies, which are often used to assist in the prediction of the design wind pressures for the cladding of buildings, (i) do physically simulate and predicts the aerodynamics effect of the actual shape of the structure by modeling building in detail, (ii) consider the directionality of the wind climate for the area where the study building is located, and (iii) overall, provide indispensable wind-effect data for the design of the cladding and structural frame work.

There is considerable research on square, rectangular and cylindrical structures (Macdonald, 1975; Meroney, 1988; Liu, 1991 and Lin, et al., 2005) but only few research studies have investigated wind pressures on irregular shapes (Cook, 1985). Stathopoulos and Zhou (1993) examined the wind loads on stepped-roof building of L-shape plan view as well as for L-shaped cross-section through a numerical study. The authors found a good agreement in the latter case between numerically and experimentally obtained results at normal wind incidence. Gomes et al. (2005) investigated the wind pressure distributions experimentally and numerically on the inner faces of L-shape and U-shape models having a scale of 1:100. The authors found general good agreement for normal wind incidence, whereas some differences have occurred for other directions. Chaudhry and Garg (2006) investigated the pressure and force coefficients of typical shape building made from four rectangular shaped blocks

arranged in a cruciform shape and it was concluded that building under consideration was subjected to significantly higher pressure coefficients as compared to the rectangular/square shape buildings.

Although L- and T- shapes are very common building configurations, experimental data for wind pressure distributions on all the sides of L-shaped models and T-shaped models having different dimensions and at different wind directions is very limited. Therefore, it is proposed to carry out wind tunnel studies on two models of L- and T-plan shape each in order to assess the effectiveness of building plan shape and wind direction in changing the wind pressure distributions. The effectiveness of shifting of upwind block from the edge of downwind block to the center of it, which transforms the L-shape into T-shape model on the pressure distribution, is also assessed. This study then attempts to provide the needful information of wind pressure distributions, mean and peak pressure coefficients on the building models having a geometrical configuration of L-plan and T-plan shape over an extended range of incidence wind direction.

2. Experimental Program

2.1 Details of models: The models used for the experiments were made of transparent perspex sheet of 6 mm thick at a geometrical model scale of 1:300. Plan area and height of all the models was kept 10000 mm^2 and 300 mm respectively for comparison purposes. The rectangular model of dimension 200 mm x 50 mm was split up in two blocks and arranged in different configurations to form the 'L' and 'T' plan shape. Model L-1 and T-1 was made from two rectangular blocks, namely block-1 of dimensions 75 mm x 50 mm and block-2 of dimensions 125 mm x 50mm. Model L-2 and T-2 was made from two rectangular blocks, namely block-1 of dimension 50 mm x 50 mm and block-2 of dimensions 150 mm x 50 mm. In case of models L-1 and L-2, block-1 was placed at the edge of block-2, whereas in case of models T-1 and T-2, block-1 was placed at the center of block-2. Plan and isometric views of the models are shown in Figure 1(a). All the models were instrumented with more than 170 numbers of pressure taps at seven different height levels of 25, 75, 125, 175, 225, 250 and 275 mm from bottom to obtain a good distribution of pressures on all the sides of models. Figure 1(b) shows the pressure tapping locations along the periphery of models. These pressure taps have been placed as near as edges of the sides to attempt to capture the high-pressure variation at the edge of the sidewalls.

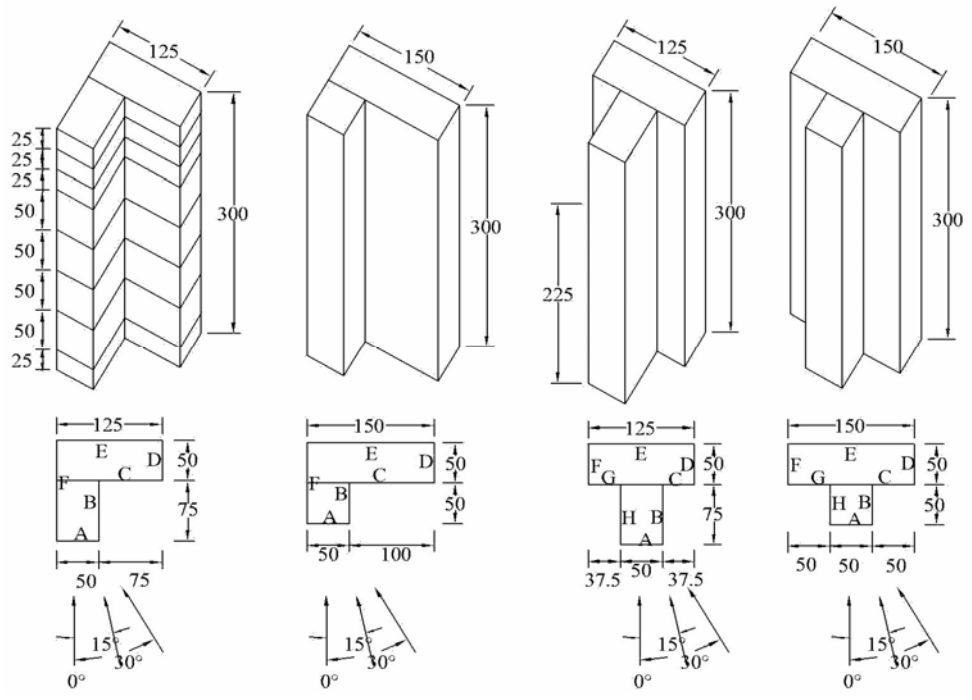

Figure 1(a) Plan and isometric views of building models (Dimensions in mm)

For making the pressure points, the steel tap of 1 mm internal diameter was inserted in to the hole drilled on the model surface such that its one end flushes to the outer side of the model surface and another end of the steel tap was connected to the vinyl tubing of 1.2 mm internal diameter and 700 mm length. The free end of vinyl tubing was connected to Baratron Pressure Gauge to measure the fluctuating wind pressures records at a particular point. The tubing system was dynamically calibrated to determine the amplitude and phase distortion. The pressure gauge provides the pressure at particular tapping on its analog scale after

adjusting it to a suitable sensitivity range, which is called Baratron range. The analog surface pressure reading from the Baratron was converted to digital reading with solid-state integrator and subsequently the mean, r.m.s., maximum and minimum pressures were recorded in the computer using the data logger. Each tap was sampled for 20 seconds at a frequency of 250 samples/sec.

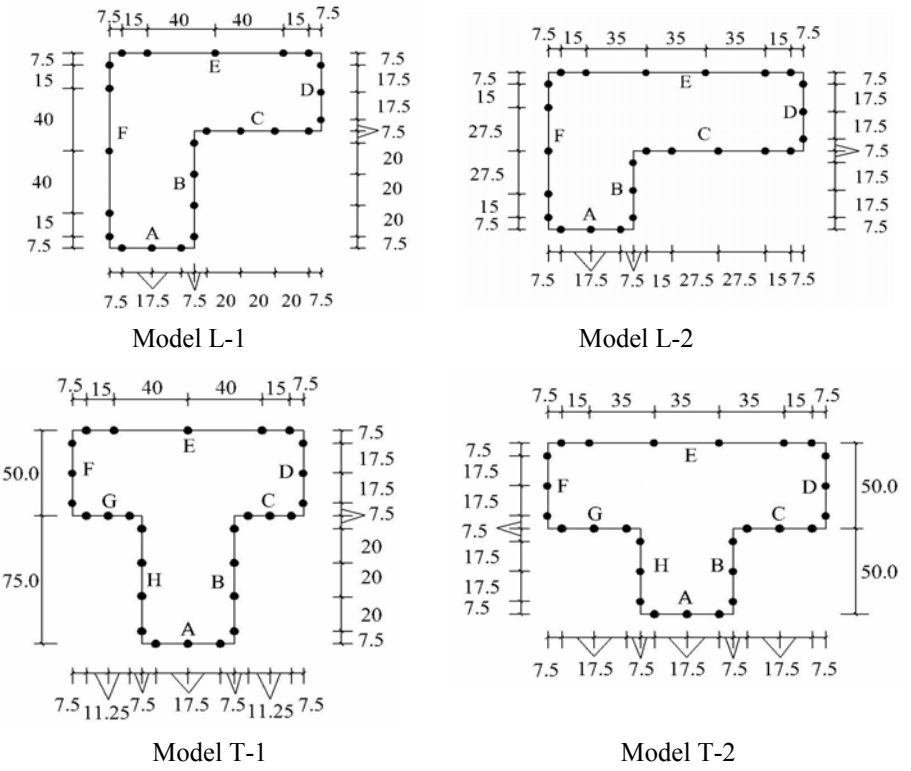

Figure 1(b) Pressure tapping locations along the periphery of models

2.2 Feature of experimental flow: The experiments were carried out in a closed circuit wind tunnel under the boundary layer flow at the Department of Civil Engineering, Indian Institute of Technology Roorkee, India. The wind tunnel has a test section of 8.2 m long with a cross sectional dimensions of 1.2 m (width) x 0.85 m (height). The experimental flow was simulated similar to the conditions of an open country terrain. Models are tested in an artificially generated gradient velocity field, which is obtained by placing the grid of horizontal bars at upstream edge of the tunnel and using roughness devices. The grid was made of 21 numbers of aluminum pipes of 9.5 mm external diameter. The bars are closely spaced near the floor and their spacing is increases as one move away from the floor. The center-to-center distance between the bars was decided based on an approach given by Gayatri (1978) to develop a boundary layer velocity profile.

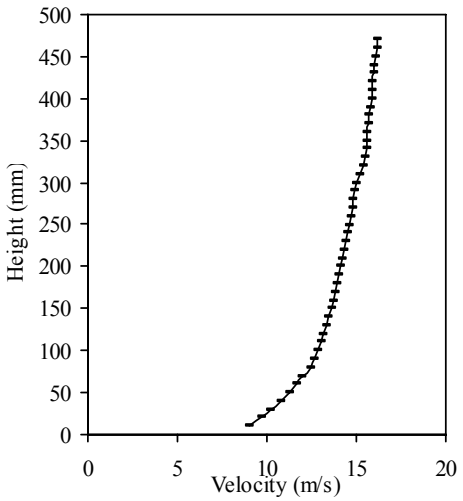

Figure 2(a) Velocity profile at the test section

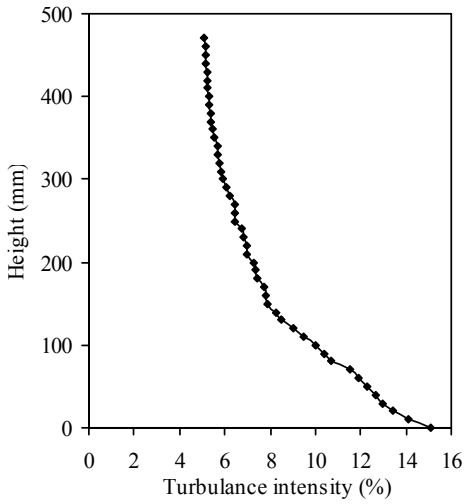

Figure 2(b) Turbulence intensity at the test section

A reference Pitot tube was located at a distance of 5.5 m from the grid and 300 mm above the floor of the wind tunnel to measure the free stream velocity. A manually controlled turn-table was installed at a distance of 6.1 m from the upstream edge of the test section. Models under the study were installed at the center of the turn-table, which can be rotated to adjust the angle of wind incidence. In the present study the reference wind velocity has been maintained as 15 m/sec at the roof level of the model. The power-law index (∞) inside the tunnel is 0.143. The gradient height for open country terrain is 300 m; and accordingly that of the simulated wind fields in the wind tunnel is 1 m. The variation of mean velocity and turbulence intensity along the height at the test section is shown in Figures 2(a) and 2(b) respectively.

3. Results and Discussion

Mean, r.m.s., maximum and minimum pressure coefficients on all the sides of L-shape and T-shape building models are evaluated from the fluctuating wind pressure records at all pressure point over an extended range of wind incidence angles of 0° to 180° at an interval of 15°. The general characteristics and observed pressure distribution on L-shape and T-shape models are summarized as follows.

3.1 L-shape building models:

Figures 3 shows the mean pressure coefficient contours of model L-1 at wind incidence angles of 0° to 75° at an interval of 15°. Figures 4 shows the similar contours for model L-2 at wind incidence angles of 0° to 120° at an interval of 15°.

Front face-A of both L-shape models is subjected to positive pressure at wind incidence angle of 0°. However, wind pressure coefficients distribution does not remain symmetrical about the vertical centerline as in the case of rectangular/square bluff body. It increases from left edge to right edge (i.e. towards the re-entrant corner) of face-A due the blockage of wind flow by face-C and subsequent stagnation of the flow in the re-entrant corner. The positive mean pressure coefficient on face-A of both the models are increases along the height due to increase in wind velocity with height. Inner faces-B and C are also subjected to positive pressures on almost all its extents. Although face-B is parallel to face-F, which is a side face, is subjected to positive pressures and not suction due to the blockage of wind flow by face-C, which causes stagnation of flow in that re-entrant corner. It is the peculiar characteristics of L-shape buildings. Note that in a single rectangular/square bluff body, the side faces would be in suction. Inner faces-B and C of model L-2 is subjected to higher pressures as compared to the pressures on corresponding faces of model L-1. The pressure on the inner faces-B and C largely depends on its relative dimensions. The magnitude of pressures on the inner face-B is increases as the dimension of face-C increases due to the higher blockage of wind flow by face-C. Inner faces of model L-1 is subjected to higher fluctuation in pressures as compared to the fluctuation on the corresponding faces of model L-2. Values of r.m.s. pressure coefficients on inner faces varies from 0.1 to 0.22 and 0.12 to 0.17 in case of model L-1 and model L-2 respectively. Side faces-D and F are subjected to negative pressures, which increases slightly from windward to leeward edge due to the separation of wind flow from the upwind corners. The leeward face-E is subjected to suction, however the variation of suction along the height and width is almost negligible. Face-E of model L-2 is subjected to slightly higher suction as compared to the suction on face-E of model L-1, due to its smaller dimension being parallel to the wind direction. Value of mean wind pressure coefficient on face-E of model L-1 and model L-2 varies from -0.45 to -0.63 and -0.53 to -0.69 respectively.

As the angle of wind incidence increases, the positive pressures on face-A is reduces. However, higher positive pressure still exists on faces B and C near the re-entrant corner. Faces B and C of both the models are subjected to mean pressure coefficients in the range of 0.35 to 0.91 and 0.42 to 0.94 at wind incidence angle of 15° and 30° respectively. Suction on face-D increases from wind incidence angle of 0° to 30° and localized peak negative pressure coefficient of -1.98 and -1.75 is observed on face-D of model L-1 and L-2 respectively at wind incidence angle of 30°. When wind blows at an angle of 45°, larger region of stagnant air is formed in the re-entrant corner of L-shape models. The size of this region is highly dependent on the slenderness of the model and the dimension of inner faces B and C. Taller the model and uniform dimension of inner faces B and C implies a larger stagnation zone in the re-entrance, as the flow tends to contour the sides rather than flow into the cavity. Beyond the wind incidence angle of 45°, face-A of both the models is subjected to suction. At wind incidence angle of 60°, face-A of model L-1 and L-2 is subjected to localize peak negative pressure coefficient of -1.95 and -1.77 respectively. Wind incidence angles of 30° to 60° depending up on the dimensions of the inner faces govern the cladding design of faces B and C. At skew wind incidence angles of 15° to 75°, the part of inner faces-B and C towards the re-entrant corners is subjected to high wind pressures.

At wind incidence angle of 90°, face-C of model L-2 is subjected to suction on major portion, due to the lower blockage of wind flow by face-B, whereas both the inner faces B and C of model L-1 are subjected to pressures of almost uniform intensity on all its extent. Face-B of model L-2 is partially submerged by the shear layers emanating from the upstream edges of face-D. Therefore inner part of face-B of model L-2 is subjected to negligible suction towards re-entrant corner, whereas its outer part is subjected to pressure of marginal intensity due to direct incidence of wind flow. Face-F of model L-2 is subjected to lower suction as compared to face-F of model L-1, due to its dimension parallel to the wind direction is large as compared to model L-1. Values of mean wind pressure coefficient on face-F of model L-1 and model L-2 varies from -0.47 to -0.70 and -0.35 to -0.48 respectively. Faces B and C of model L-2 are subjected to higher fluctuating pressures and these faces are subjected to r.m.s. pressure coefficients in the range of 0.07 to 0.20 and 0.09 to 0.23 respectively.

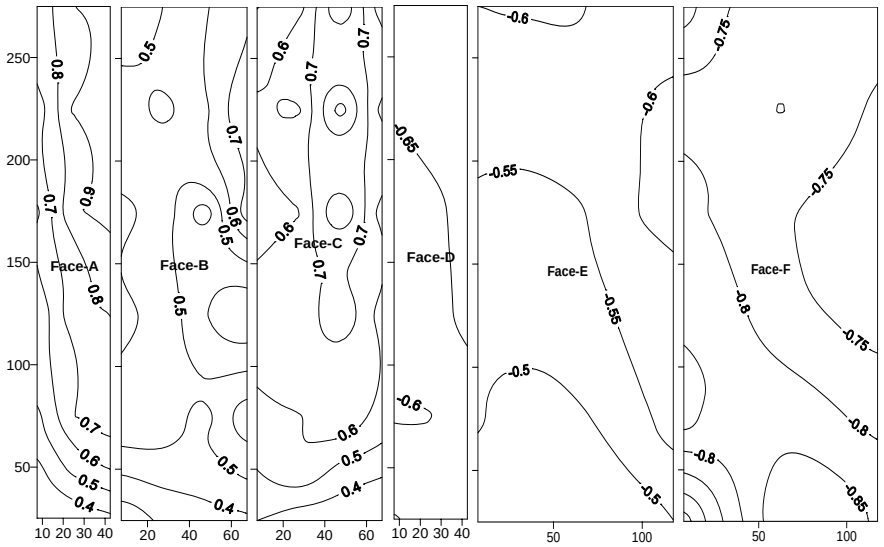

Figure 3(a) Mean surface pressure coefficient distribution- Model-L-1 (Angle-0°)

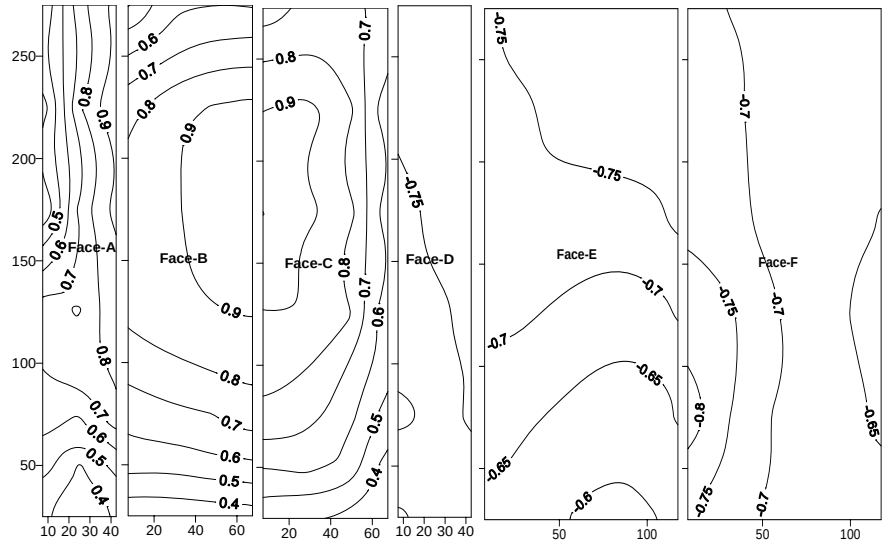

Figure 3(b) Mean surface pressure coefficient distribution- Model-L-1 (Angle-15°)

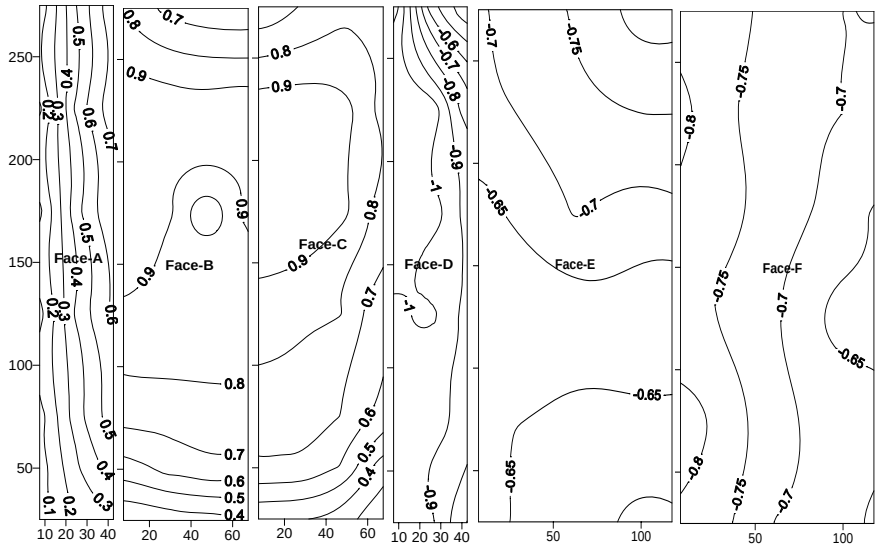

Figure 3(c) Mean surface pressure coefficient distribution- Model-L-1 (Angle-30°)

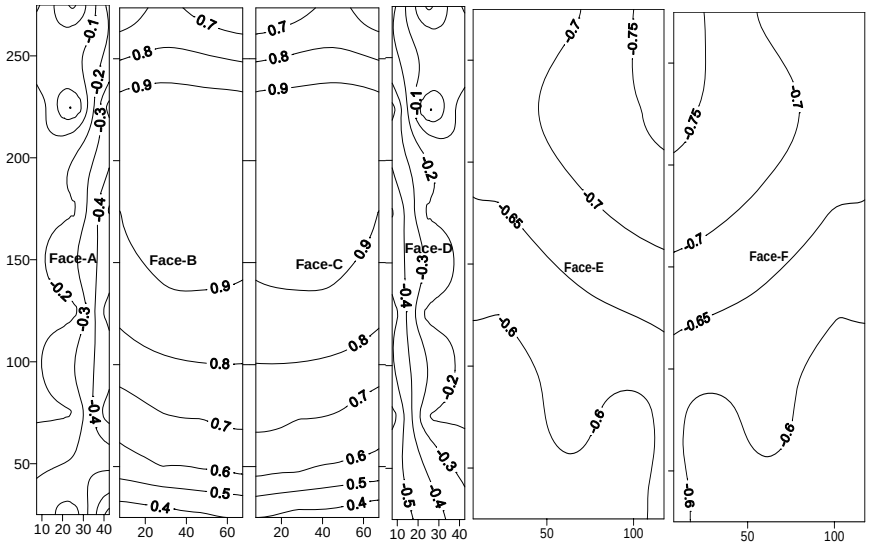

Figure 3(d) Mean surface pressure coefficient distribution- Model-L-1 (Angle-45°)

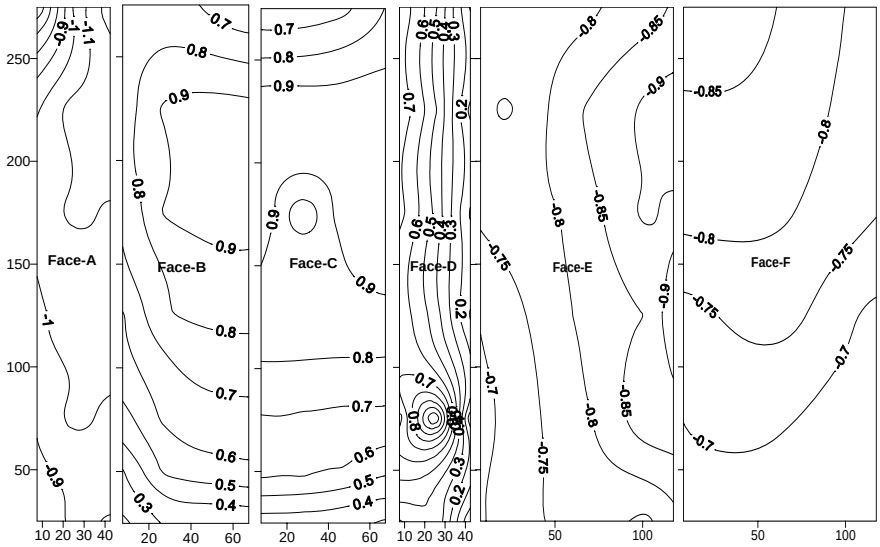

Figure 3(e) Mean surface pressure coefficient distribution- Model-L-1 (Angle-60°)

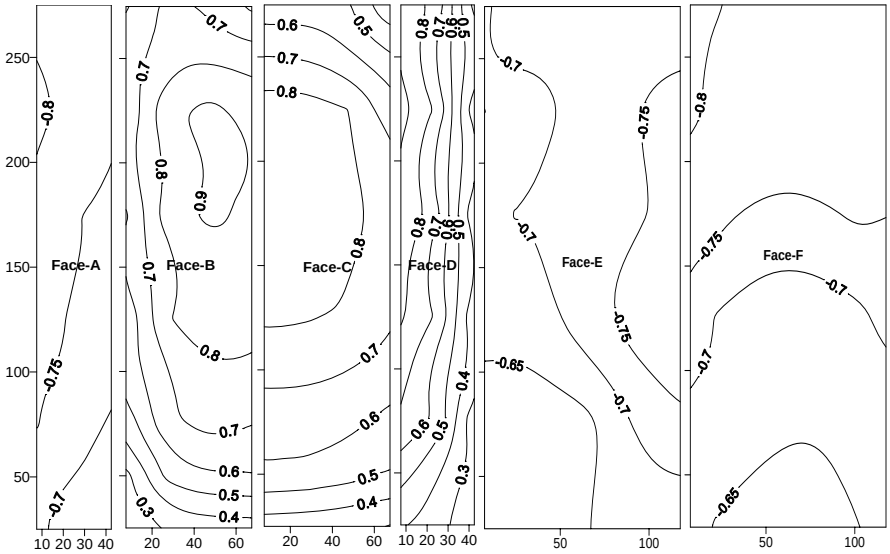

Figure 3(f) Mean surface pressure coefficient distribution- Model-L-1 (Angle-75°)

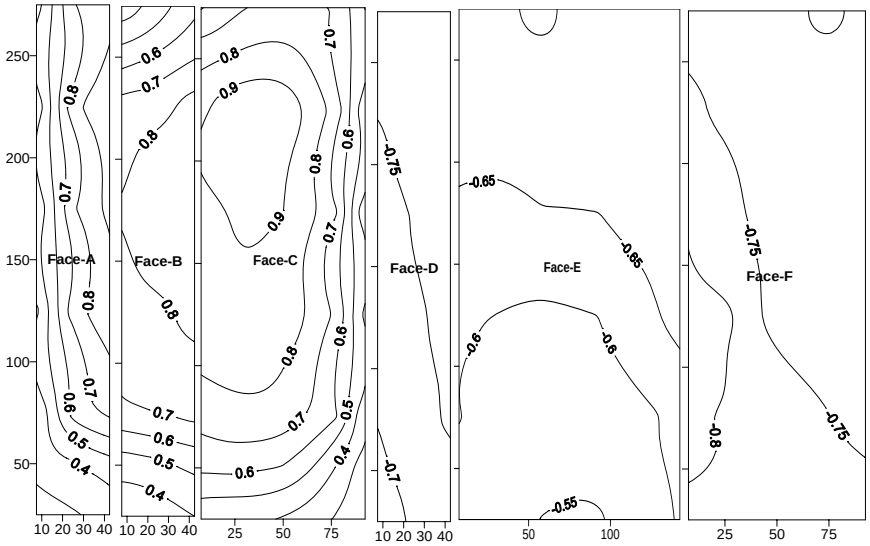

Figure 4(a) Mean surface pressure coefficient distribution- Model-L-2 (Angle-0°)

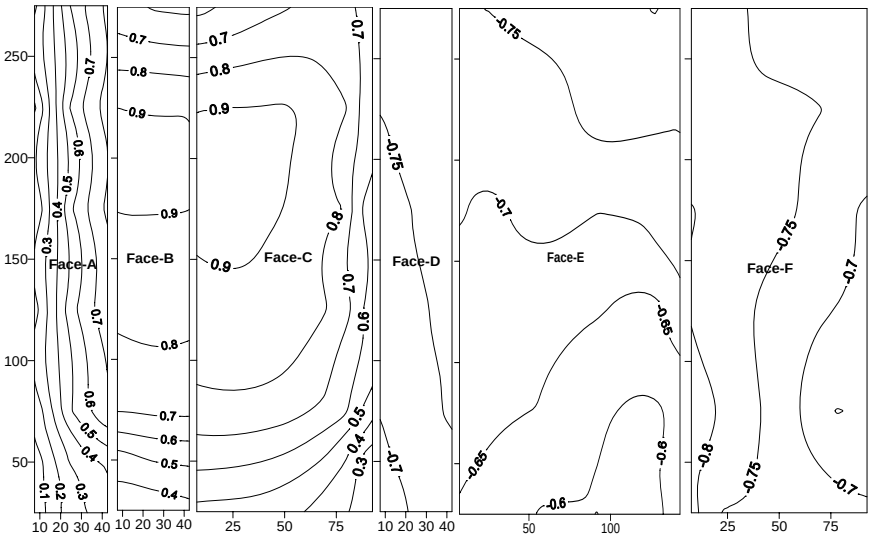

Figure 4(b) Mean surface pressure coefficient distribution- Model-L-2 (Angle-15°)

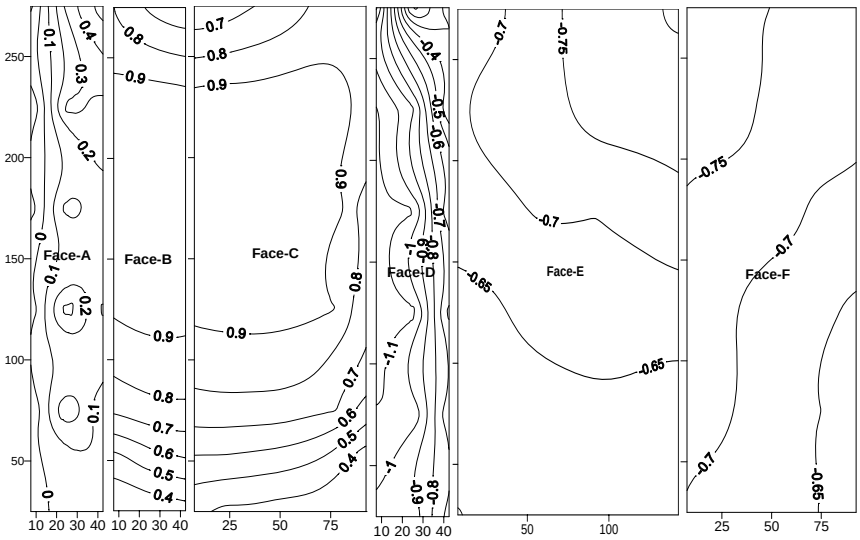

Figure 4(c) Mean surface pressure coefficient distribution- Model-L-2 (Angle-30°)

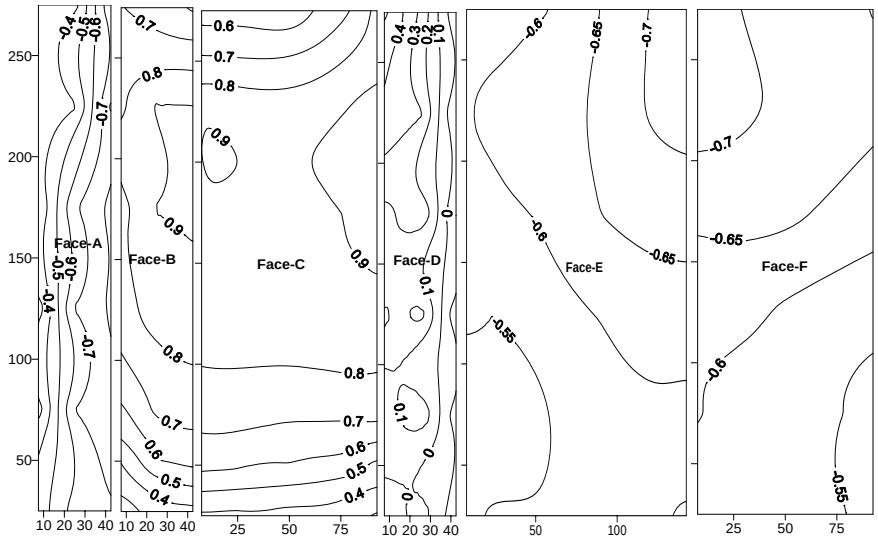

Figure 4(d) Mean surface pressure coefficient distribution- Model-L-2 (Angle-45°)

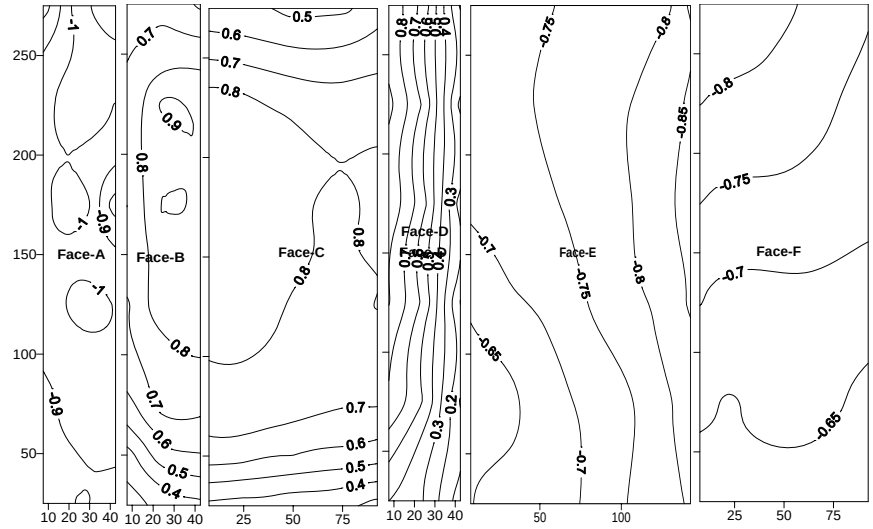

Figure 4(e) Mean surface pressure coefficient distribution- Model-L-2 (Angle-60°)

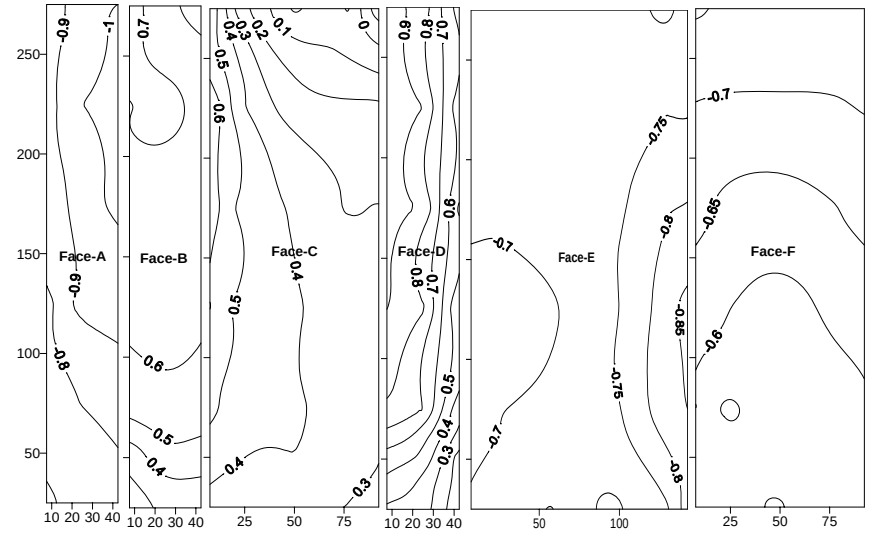

Figure 4(f) Mean surface pressure coefficient distribution- Model-L-2 (Angle-75°)

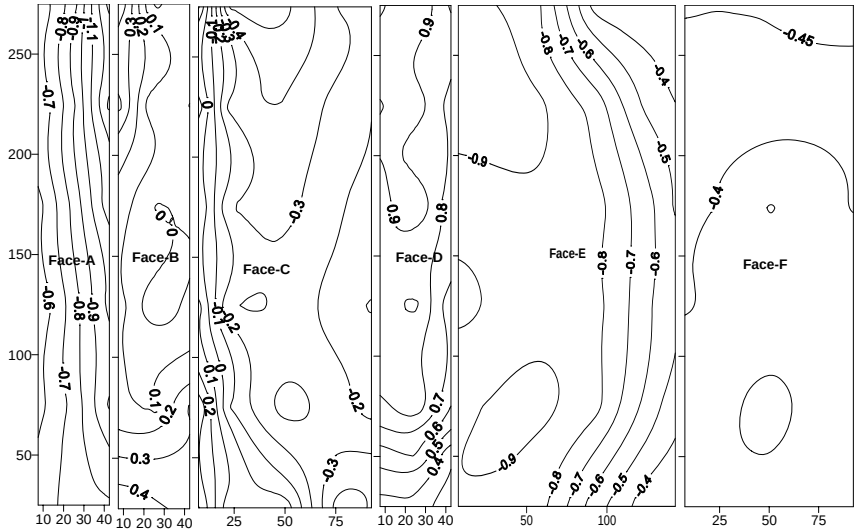

Figure 4(g) Mean surface pressure coefficient distribution- Model-L-2 (Angle-90°)

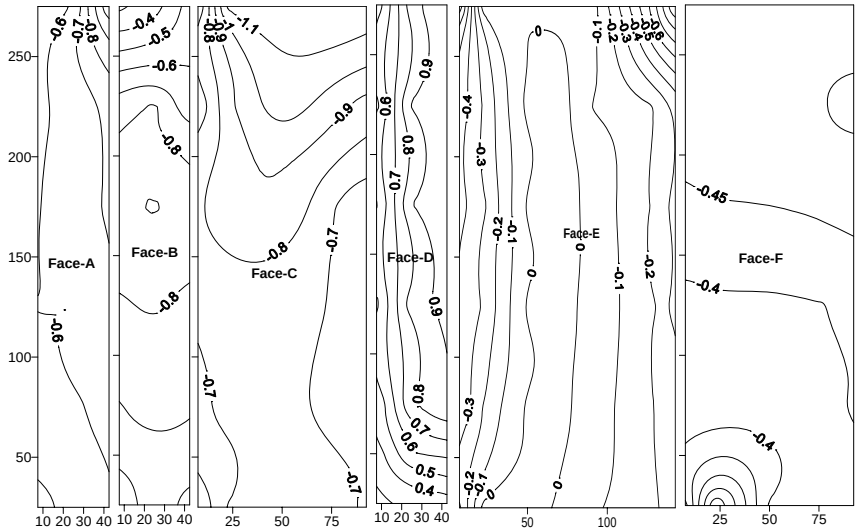

Figure 4(h) Mean surface pressure coefficient distribution- Model-L-2 (Angle-105°)

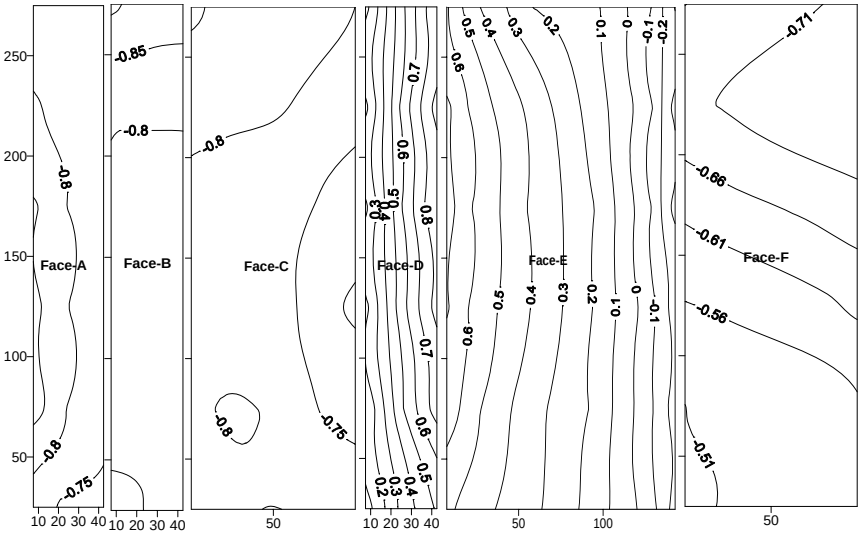

Figure 4(i) Mean surface pressure coefficient distribution- Model-L-2 (Angle-120^0)

At wind incidence angle of 105°, Inner part of face-B of model L-1 is subjected to suction, whereas positive pressures on the outer part of face-B are increases due to the direct incidence of flow on that small area after skipping over the opposing wing. However, face-B of model L-2 is submerged by the shear layers emanating from the upstream edge/block; hence it is subjected to suction almost all its extent. Faces B and C of model L-2 are subjected to a localized peak negative pressure coefficient of -1.8 and -2.01 respectively. Faces B and C of both the models are subjected to highly fluctuating pressures at wind incidence angle of 105° and 120°, and these faces subjected to r.m.s. pressure coefficients in the range of 0.05 to 0.38. At wind incidence angle of 120° to 180°, inner faces B and C of both the models are not directly exposed to the flow, being rather under the wake region influence. As a consequence, the pressure coefficient distribution is negative (suction) and almost uniform.

When wind incidence angle is 180° i.e. normal to face-E, the wind flow around both the models is very similar to that of rectangular blocks in the upwind region. However the flow patterns are totally different in the downwind region. There is a large and non-symmetrical vortex formed in the L–cavity with smaller vortices formed behind the downward back wall of the wings/block-1 of the models, unlike the two symmetrical vortices in case of rectangular bluff body. Face-E of both the model is subjected to maximum mean wind pressure coefficients of 0.85, whereas all the remaining five faces of both the models are subjected to mean pressure coefficient in the range of -0.42 to -0.92 without any significant changes across the section.

Influence of wind incidence angle on wind pressure values on inner face-B of L-shaped building models are shown in Figures 5(a) and 5(b). It is observed from Figures 5(a) and 5(b) that the wind incidence angle has great influence on the pressure values. At the same section on the model, mean pressure coefficients varies from -0.8 to 0.95 approximately when wind incidence angle changes from 0° to 180°. Further it is noticed that, suction does not vary with height appreciably, whereas pressure values increase with height of the building. The stagnation point, where the value of mean $C_{p,mean}$ reaches a maximum, is approximately at about 0.8 h, where h is the height of the model. Contours for other wind directions are not shown due to paucity of space.

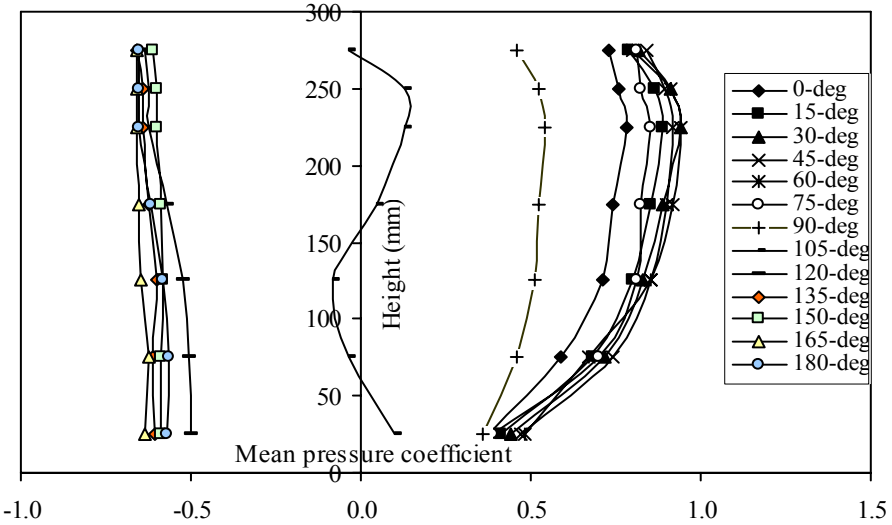

Figure 5(a) Mean pre. coeff. at a distance of 7.5 mm from re-entrant corner on face-B (model L-1)

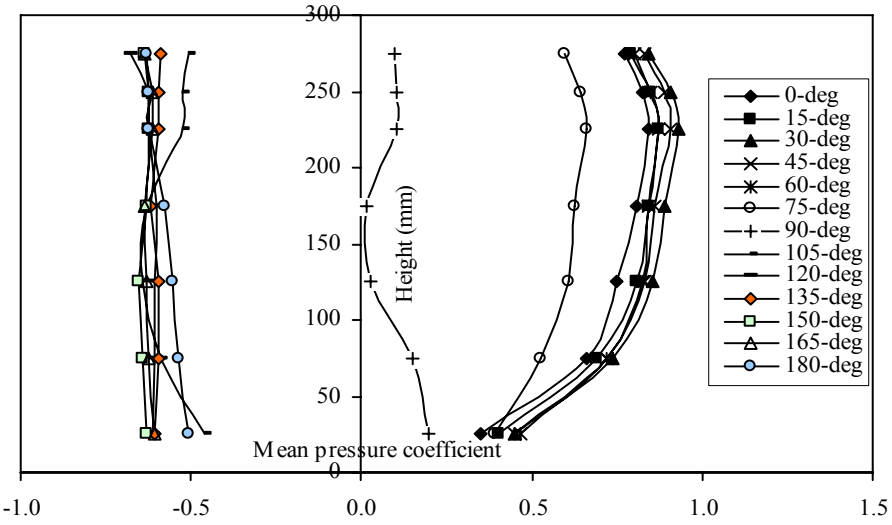

Figure 5(b) Mean pre. coeff. at a distance of 7.5 mm from re-entrant corner on face-B (model L-2)

3.2 T-shape building models: Figures 6 shows the mean pressure coefficient contours of model T-1 at wind incidence angles of 0° to 120° at an interval of 15°. Figures 7 shows the similar contours for model T-2.

Since the flow is symmetrical when the wind incidence angle is 0°, i.e. wind direction perpendicular to face-A, the stagnation point is in the middle of front face-A. Face-A of both the models is subjected to positive pressures and values of mean pressure coefficients are varies in the range of 0.3 to 0.92. Side faces-B and H of model T-1 are subjected to negative pressures, whereas the corresponding faces of model T-2 are subjected to positive pressures. This phenomenon is attributed to the blockage of wind flow by face-C, which causes stagnation of flow in that re-entrant corner of model T-2, whereas face-B and face-H of model T-1 is partially submerged by the shear layers emanating from the upstream edge/block, thus these faces is subjected to suction. The exterior part of face-C and G of model T-1 is subjected to positive wind pressures due to direct incidence of flow on that small area and the portion towards the re-entrant corner of face-C is still subjected to suction, whereas the entire face-C and G of model T-2 is subjected to positive pressures. The distribution and magnitude of wind pressure coefficients on face-B is highly affected by the width of face-C. Face-B and face-C of model T-1 is subjected to higher fluctuating pressures as compared to the corresponding faces of model T-2. Values of r.m.s pressure coefficients on inner faces of model T-1 and model T-2 varies from 0.2 to 0.45 and 0.09 to 0.22 respectively. Side faces-D, F and leeward face-E of both the models are subjected to negative pressures. The dimension of building models significantly affects the suction on the leeward and side faces. The pressures on side face-D of model T-1 is decreases from windward to leeward side, whereas pressures on face-D of model T-2 remains almost uniform. The negative pressures on the leeward face-E are uniformly distributes, being under the wake region influence. Two symmetrical vortices are formed in the wake region of the models on downstream side. Face-E of model T-2 (-0.45 to -0.64**)** is subjected to higher suction as compared to the corresponding face of model T-1 (-0.34 to -0.46**)**, due to its dimension parallel to the wind direction is smaller as compared to model T-2.

At wind incidence angle of 15°, inner faces B and C of both the models are subjected to higher pressures as compared to pressures on the corresponding faces at wind incidence angle of 0°. As wind incidence angle increases, the mean pressure coefficients on faces B and C increases up to 45° and 30° in case of models T-1 and T-2 respectively. Beyond the wind incidence angle of 30°, faces G and H of both the models being under the wake region influence. As a consequence, the pressure coefficient distribution on these faces is negative and almost uniform. As wind incidence angle increases, the suction on face-E is also increases. Face-E of models T-1 and T-2 is subjected to a localized peak pressure coefficient of -1.21 and -1.5 respectively at wind incidence angle of 90°. At wind incidence angle of 90°, face-D of both the models is subjected to positive pressure. However, wind pressure coefficients distribution does not remain symmetrical as in the case of rectangular/square bluff body. It increases from outer edge to the edge towards the re-entrant corner. Inner faces B and C are also subjected to positive pressures on almost all its extents, due to blockage of wind flow by face-B, which causes stagnation of flow in that re-entrant corner. Face-C of model T-1 is subjected to higher mean pressure coefficients (0.34 to 0.82) as compared to the corresponding face-C of model T-2 (0.2 to 0.55), due to the larger width of face-B of model T-1. Faces G and H of both the models are not directly exposed to the flow, being rather under the wake region influence. As a consequence, the pressure coefficient distribution on these faces is negative and these faces are subjected to mean pressure coefficients in the range of -0.40 to -0.61.

At wind incidence angle of 105°, the outer part of face-B of model T-2 is subjected to positive pressure, whereas the inner part of face-B towards the re-entrant corner and entire face-C is under the wake region influence hence it is subjected to suction. This can be attributed to the direct incidence of flow on that small outer area of face-B, after skipping over the opposing wing. Face-B and C of model T-1 is subjected to positive pressures on almost all its extent, because of the larger width of face-B and smaller width of face-C. Face-B of model T-1 and model T-2 is subjected to mean pressure coefficients in the range of 0.2 to 0.85 and -0.15 to 0.75 respectively. Whereas face-C of models T-1 and T-2 is subjected to mean pressure coefficients in the range of 0.3 to 0.64 and -0.40 to -0.60 respectively. Face-C of model T-1 and model T-2 is subjected to r.m.s. pressure coefficients in the range of 0.09 to 0.33 and 0.06 to 0.42 respectively.

At wind incidence angle of 120°, inner part of face-B towards the re-entrant corner and entire face-C of model T-1 is being under the wake region and is subjected to suction. Whereas the outer half part of face-B of model T-1 is subjected to positive pressures due to the direct incidence of flow on that it, after skipping over the opposing wing/block. Faces B and C of model T-2 are subjected to a peak negative pressure coefficients of -2.1 and –2.01 respectively. At wind incidence angle between 135° and 180°, inner faces (face-B, C, G & H) of both the models are not directly exposed to the flow, being rather under the wake region influence. As a consequence, the pressure coefficient distribution is negative and almost uniform.

At wind incidence angle of 180°, i.e. normal to face-E, the distribution of pressure coefficients and hence wind flow around both the models is very similar to that of rectangular blocks in the upwind region. However the flow patterns are totally different in the downwind region. Two symmetrical vortices would be formed on either side of central wing/block of T-shaped model on downwind side. Face-E of both the models is subjected to positive pressures, whereas all the remaining faces of both the models are subjected to mean pressure coefficients in the range of -0.40 to -0.90 without any significant changes along the height. Variation of mean wind pressure coefficients along the height at a distance of 7.5 mm from the re-entrant corner on face-B of models T-1 and T-2 are shown in Figures 8(a) and 8(b) respectively. It is observed that the wind incidence angle has great influence on the pressure values. At the same section on the model, mean pressure coefficients varies from -0.8 to 0.95 approximately, when wind incidence angle changes from 0° to 180°. Further it is noticed that pressure values increase with height of the building, whereas suction does not vary with height appreciably.

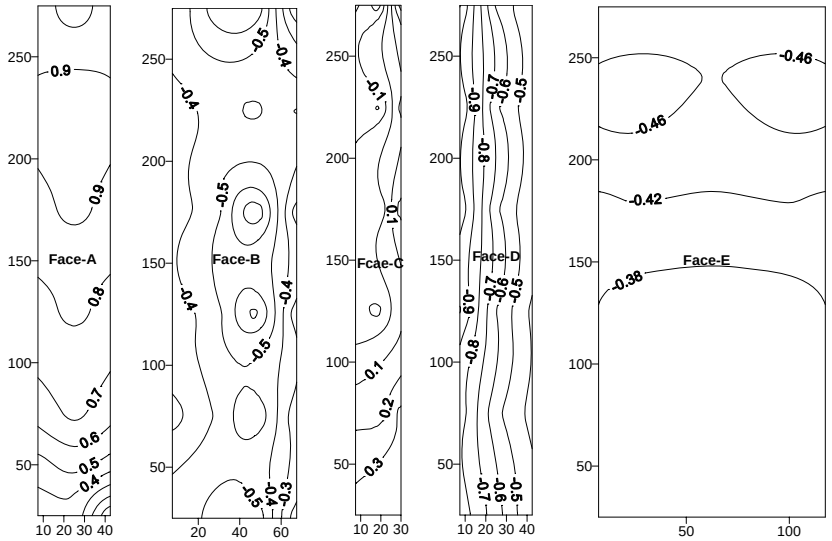

Figure 6(a) Mean surface pressure coefficient distribution- Model-T-1 (Angle-0°)

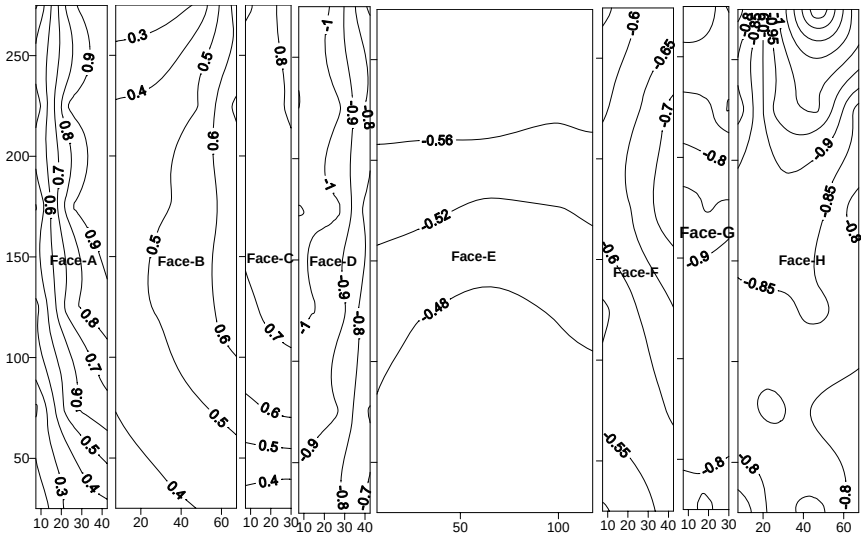

Figure 6(b) Mean surface pressure coefficient distribution- Model-T-1 (Angle-15°)

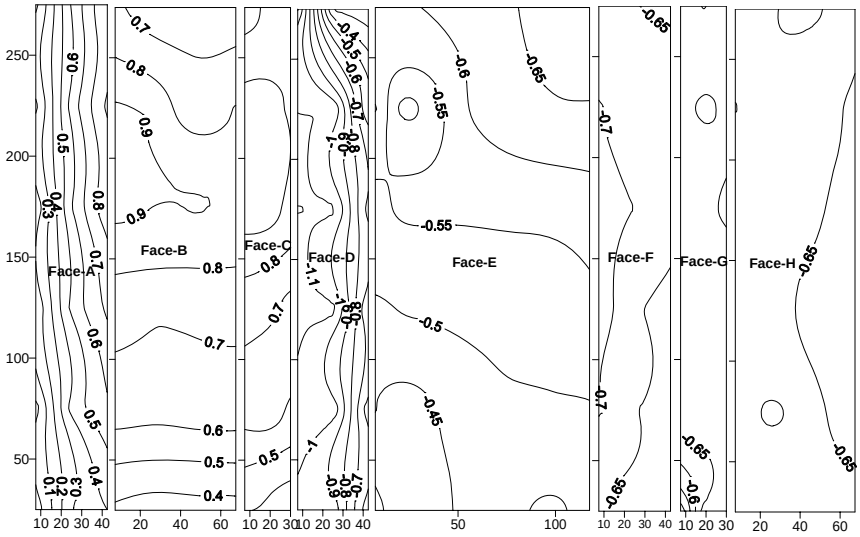

Figure 6(c) Mean surface pressure coefficient distribution- Model-T-1 (Angle-30°)

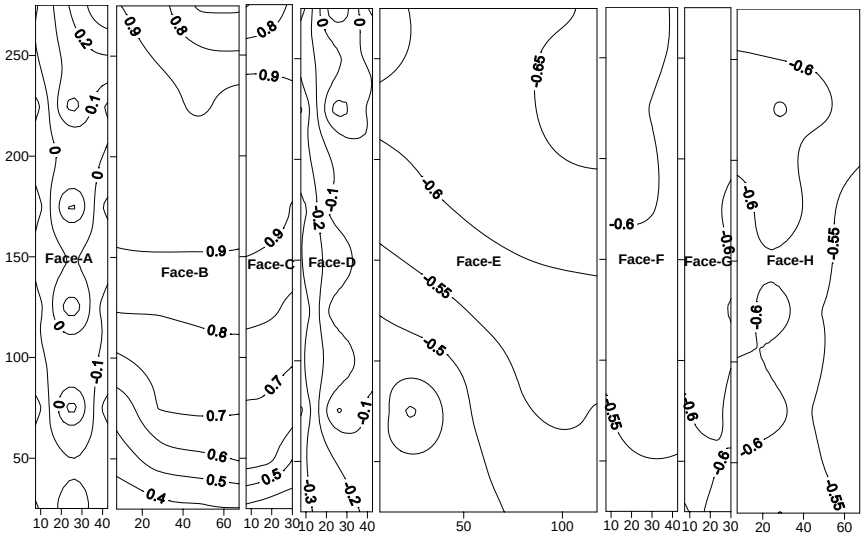

Figure 6(d) Mean surface pressure coefficient distribution- Model-T-1 (Angle-45°)

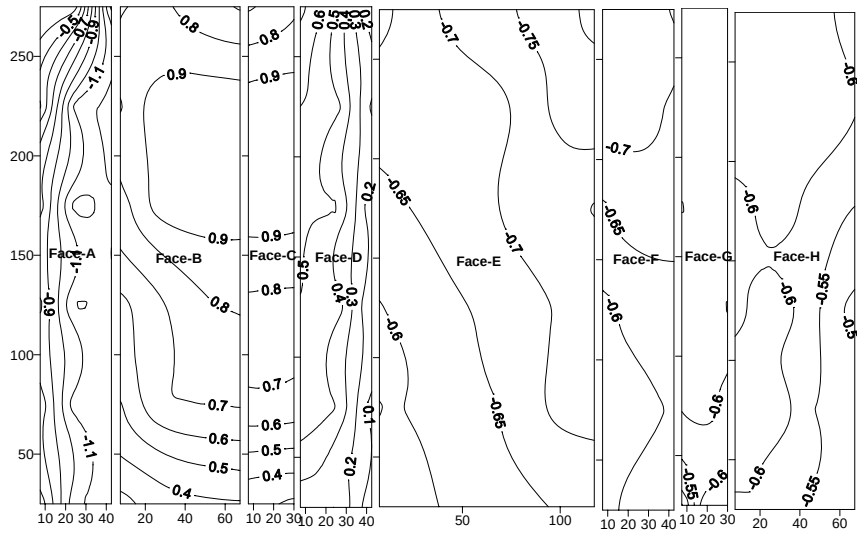

Figure 6(e) Mean surface pressure coefficient distribution- Model-T-1 (Angle-60°)

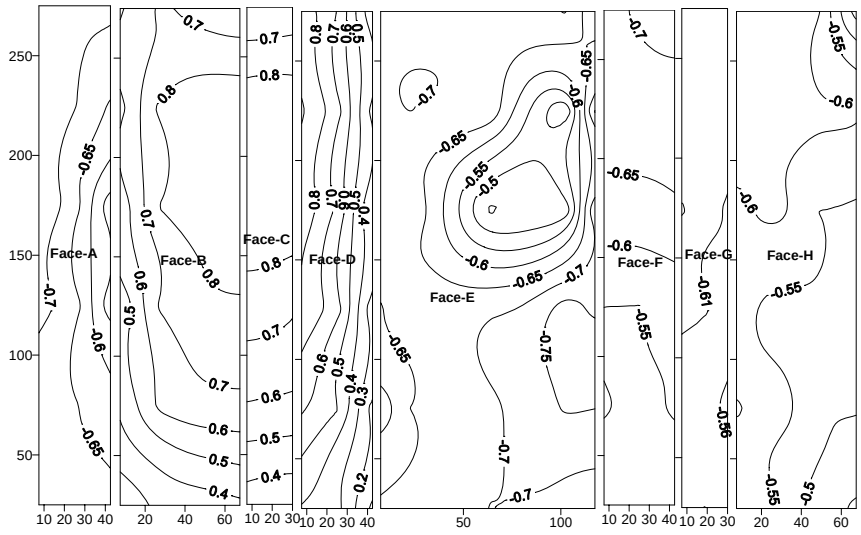

Figure 6(f) Mean surface pressure coefficient distribution- Model-T-1 (Angle-75°)

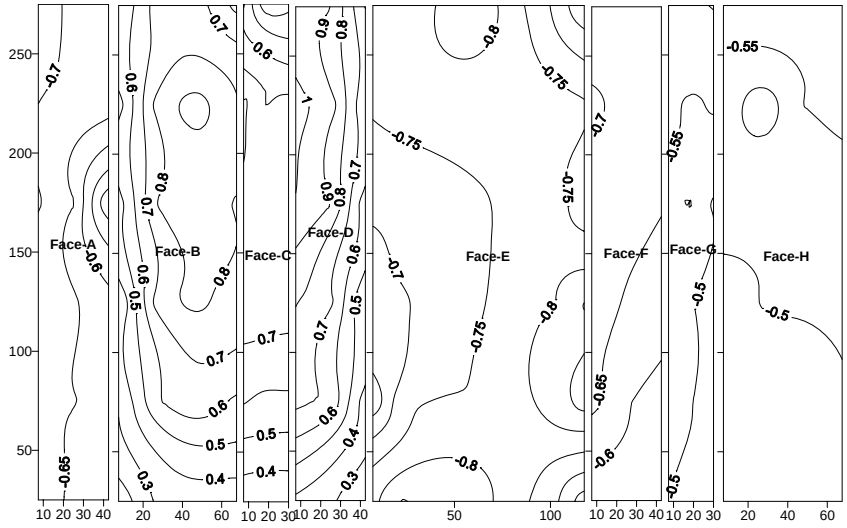

Figure 6(g) Mean surface pressure coefficient distribution- Model-T-1 (Angle-90°)

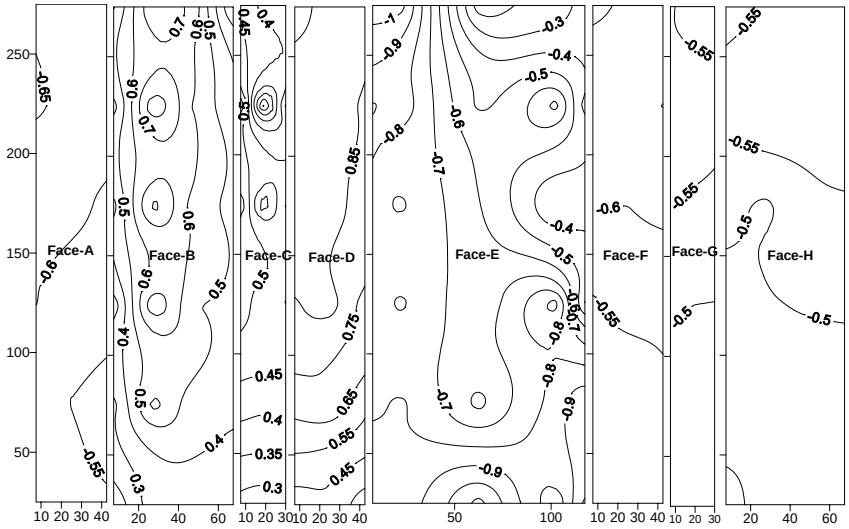

Figure 6(h) Mean surface pressure coefficient distribution- Model-T-1 (Angle-105°)

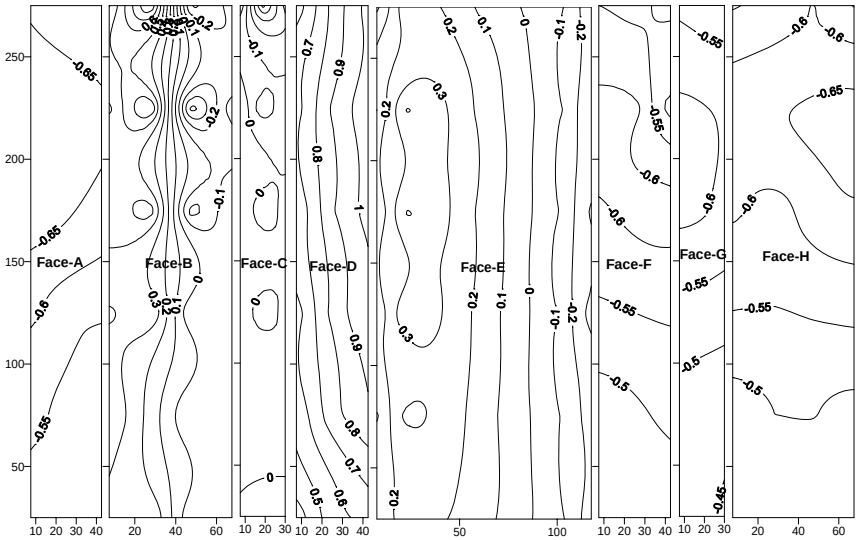

Figure 6(i) Mean surface pressure coefficient distribution- Model-T-1 (Angle-120^0)

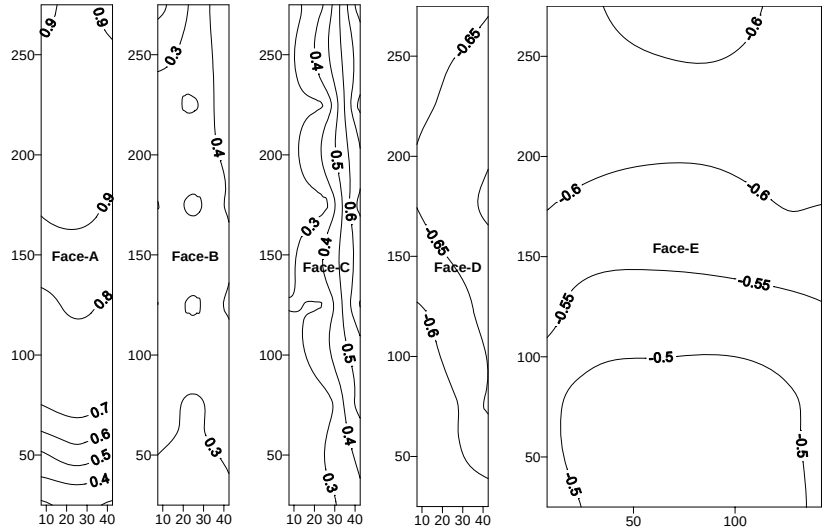

Figure 7(a) Mean surface pressure coefficient distribution- Model-T-2 (Angle-0°)

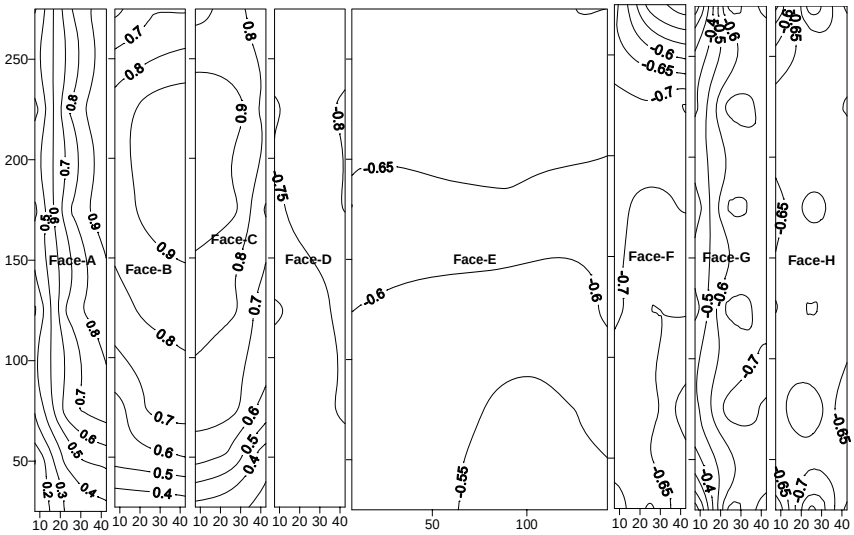

Figure 7(b) Mean surface pressure coefficient distribution- Model-T-2 (Angle-15°)

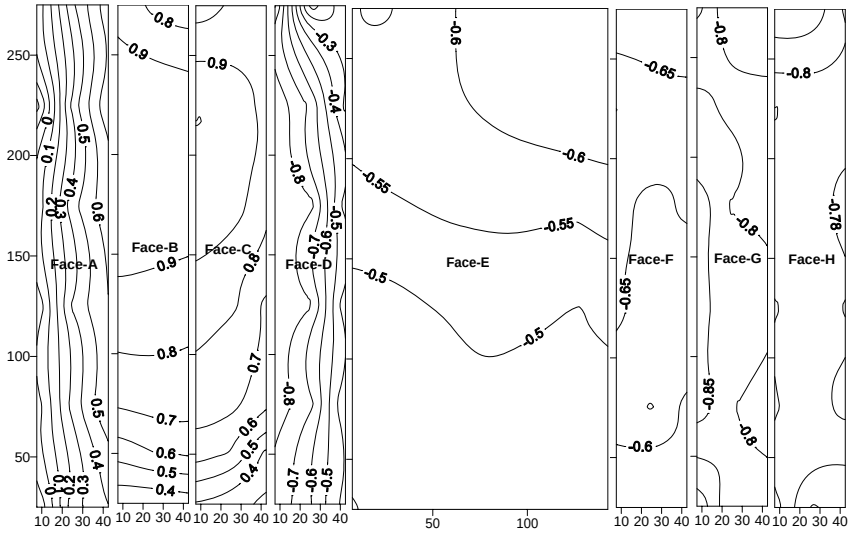

Figure 7(c) Mean surface pressure coefficient distribution- Model-T-2 (Angle-30°)

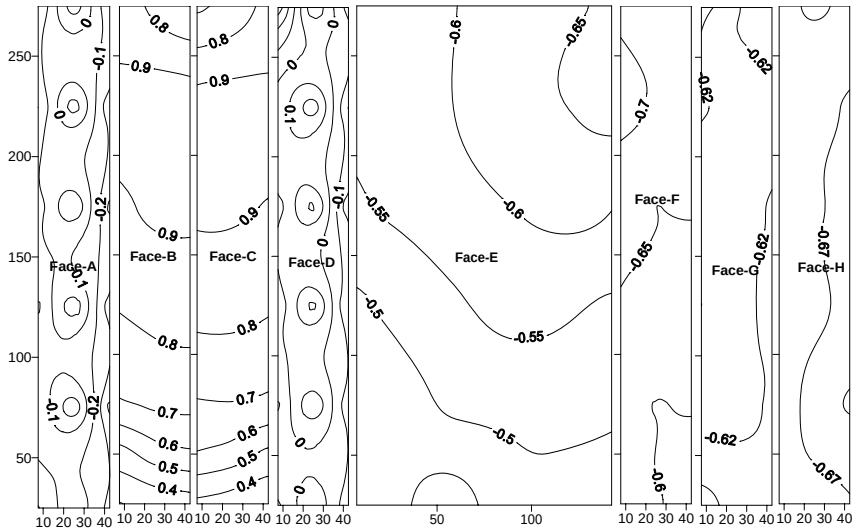

Figure 7(d) Mean surface pressure coefficient distribution- Model-T-2 (Angle-45°)

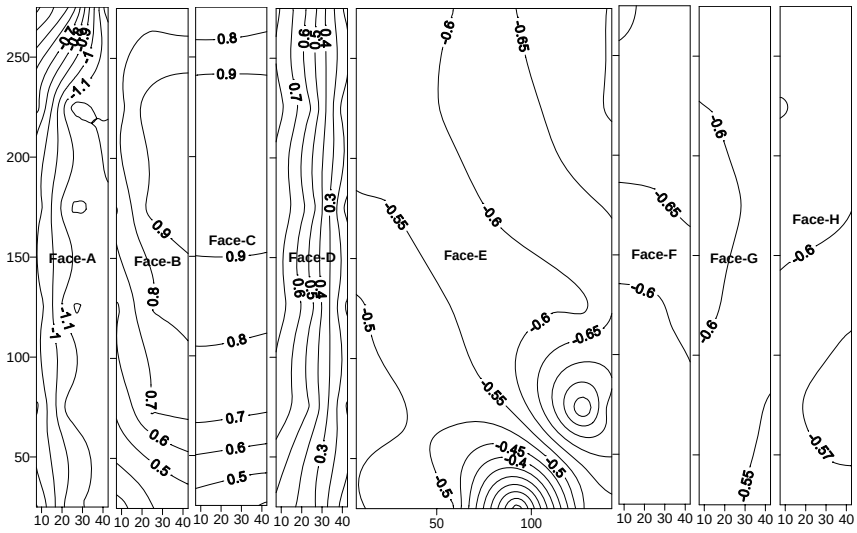

Figure 7(e) Mean surface pressure coefficient distribution- Model-T-2 (Angle-60°)

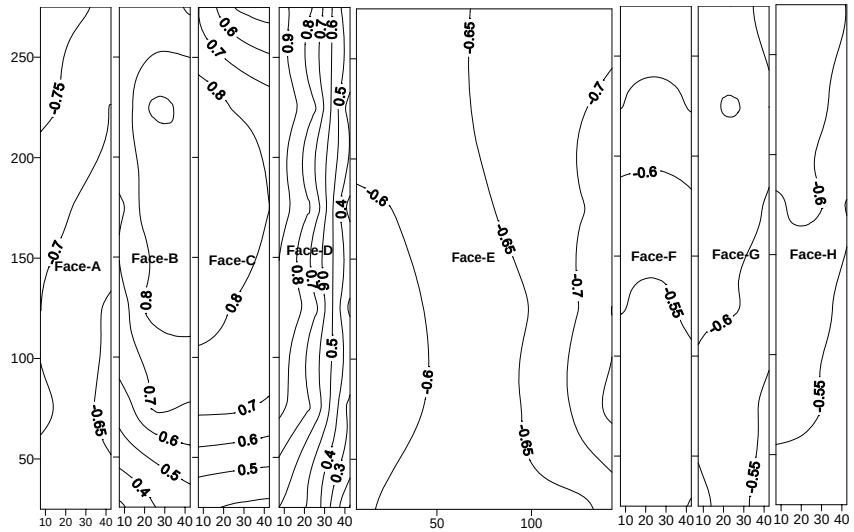

Figure 7(f) Mean surface pressure coefficient distribution- Model-T-2 (Angle-75°)

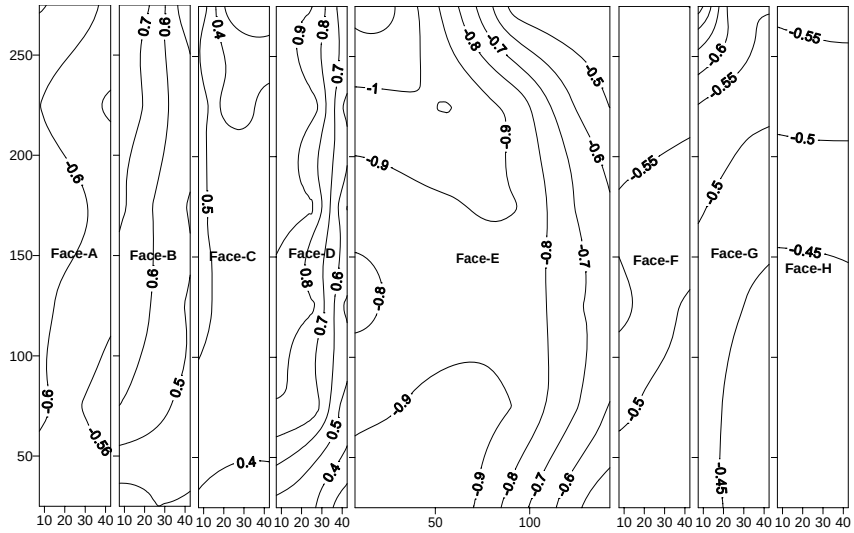

Figure 7(g) Mean surface pressure coefficient distribution- Model-T-2 (Angle-90°)

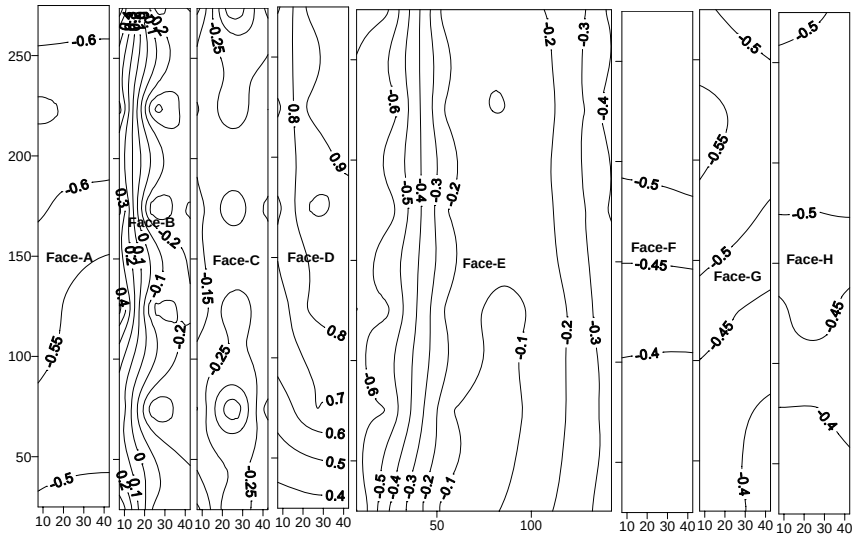

Figure 7(h) Mean surface pressure coefficient distribution- Model-T-2 (Angle-105°)

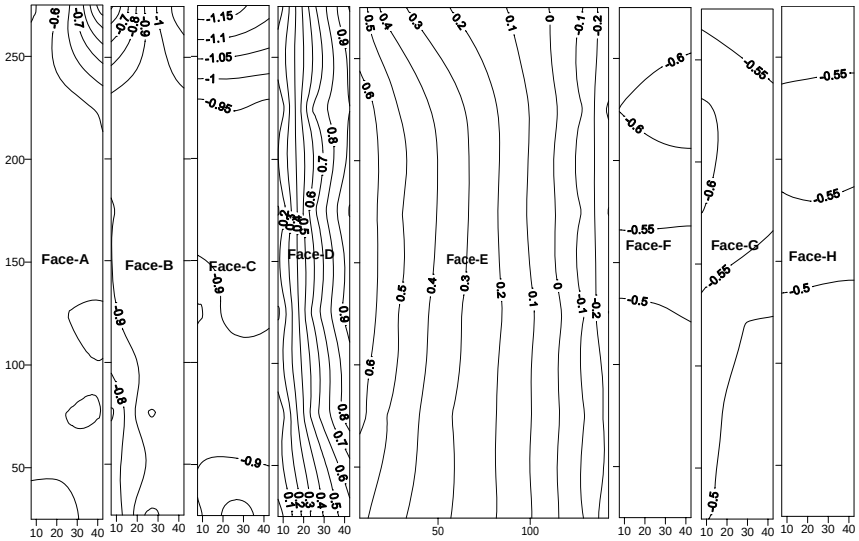

Figure 7(i) Mean surface pressure coefficient distribution- Model-T-2 (Angle-120^0)

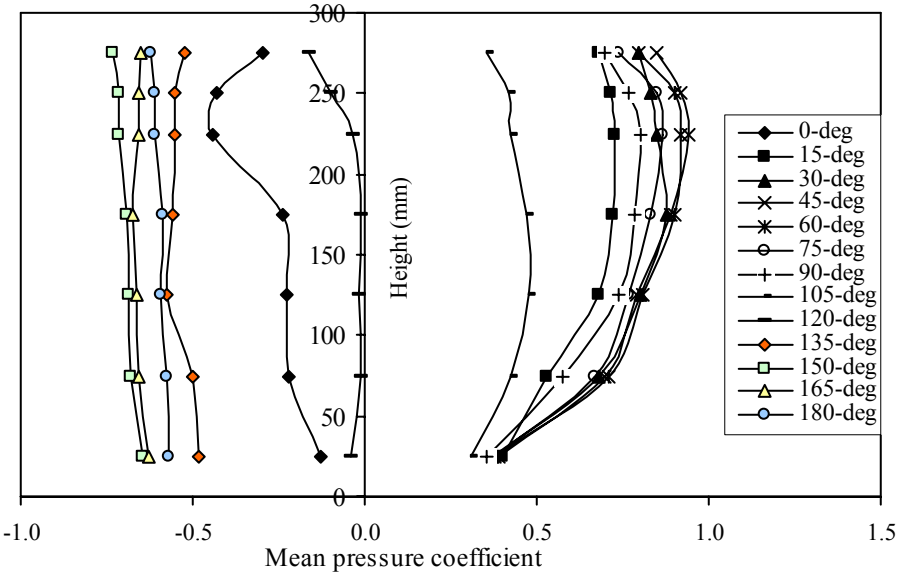

Figure 8(a) Mean pre. coeff. at a distance of 7.5 mm from re-entrant corner on face-B (model T-1)

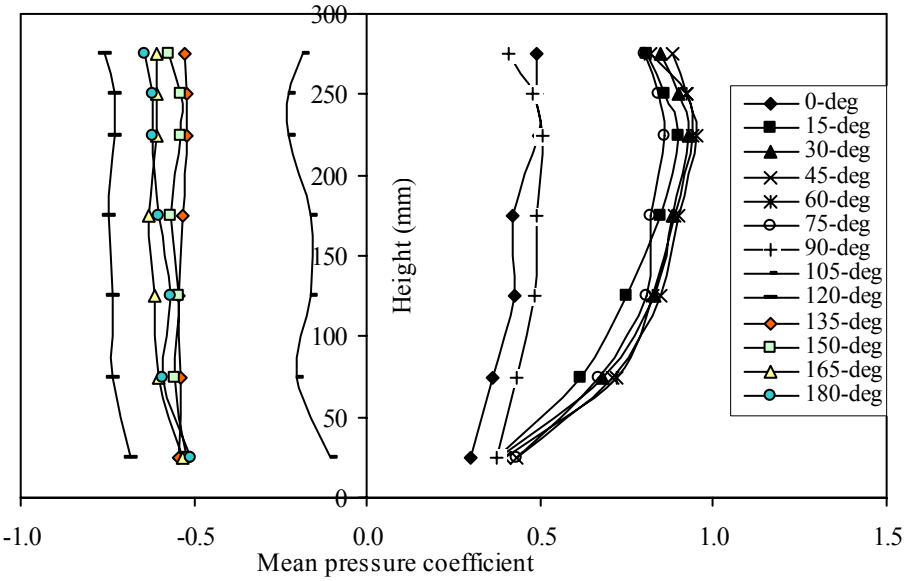

Figure 8(b) Mean pre. coeff. at a distance of 7.5 mm from re-entrant corner on face-B (model T-2)

4. Conclusions

The present study has shown that wind orientation induces different pressure distributions on the walls of L- and T-shaped models from those of isolated rectangular/square models. The influence of changing the position of upwind block from edge of the downwind block to center of it, which transforms L-shape into T-shape model, is noticeable on the pressure distribution. At 0° wind incidence angle, wind pressure distribution on face-A of L-shaped models is not remain symmetrical and highest positive pressures are moves position near the re-entrant corner due to blockage of wind flow from re-entrant corner, whereas it is almost symmetrical on face-A of T-shaped model. Inner faces B and C of L-shaped models are subjected to higher wind pressures as compared to corresponding faces of T-shaped models. Face-B of model T-2 is subjected to pressure, whereas face-B of model T-1 is subjected to suction. The distribution and magnitude of wind pressure coefficients on inner faces B and C of L- and T-shaped are significantly influenced by the interference/disturbance of the streamlines from the upwind block, plan-shape and dimension of models and wind orientations. The suction on side faces and leeward faces are also significantly affected by the plan-shape of the models and wind orientation.

At skew wind incidence angles, inner faces-B and C of L- and T-shaped models are subjected to higher pressures and its magnitude depends on the relative dimensions of face-B and C. A region of stagnation air, in which pressure rises to the stagnant values, occurs in the re-entrant corner of L- and T-shaped models at skew wind angles. The size of this region is highly dependent on the slenderness of the model and the dimension of inner faces. As the angle of incidence wind increases beyond 120°, inner faces of L- and T-shaped models are not directly exposed to the flow, being rather under the wake region influence. As a consequence, the pressure coefficient distribution is negative and almost uniform. At wind incidence angle is 180°, the wind flow around L- and T-shaped models is very similar to that of rectangular blocks in the upwind region. However the flow patterns are totally different in the downwind region.

References

Amin, J.A. 2008. Effects of plan shape on wind-induced responses of tall buildings. *Ph.D. Thesis*, Department of Civil Engineering, Indian Institute of Technology, Roorkee, India.

Chaudhry, K.K. and Garg, R. K. 2006. Wind induced flow-field study for designing cruciform shaped buildings. *Proc. of the Third National Conference on Wind Engineering*, Kolkata, India, pp.414-421.

Cook, N.J. 1985. *The designers guide to wind loading of building structures, Part-2: static structures*. Butterworths Press, London.

Gayatrri, K.S. 1978. A note on the computation of spacing betweens the rods of wind tunnel velocity-profile grid. *IWTR No. 143*, Department of Aeronautical Engineering, Indian Institute of Science, Bangalore, India.

Gomes, M.G., Rodriques, A. M. and Mendes, P. 2005. Experimental and numerical study of wind pressures on irregular-plan shapes. *Journal of Wind Engineering and Industrial Aerodynamics*, Vol. 93, pp. 741-756.

Henry Liu, 1991. Wind Engineering- A handbook for Structural Engineers. *Prentice hall*, Englewood Cliffs, New Jersey.

Lin, N., Letchford, C., Tamura, Y., Liang, B. and Nakamura, O. 2005. Characteristics of wind forces acting on tall buildings. *Journal of Wind Engineering and Industrial Aerodynamics*, Vol. 93, pp. 217-242.

Macdonald, A.J. 1975. Wind loading on buildings. *Applied Science Publishers Ltd*., London, 72.

Meroney, R.N. 1988. Wind tunnel modeling of the flow about bluff bodies. F.R.G. Aachen (Ed.), Advances in Wind Engineering, *Proc. of the Seventh International Congress on Wind Engineering*, Part-2, Elsevier, Amsterdam, pp. 203-223.

Stathopoulos, T. and Zhou, Y. 1993. Numerical simulation of wind induced pressures on buildings of various geometries. *Journal of Wind Engineering and Industrial Aerodynamics*, Vol. 46/47, pp. 419-430.

Suresh Kumar, K., Irwin, P.A. and Davies, A. 2006. Design of tall buildings for wind: Wind tunnel vs. Codes/standards. *Proc. of the Third National Conference on Wind Engineering*, Calcutta, India, pp. 318-325.

Biographical notes

J.A. Amin received Ph.D. from Indian Institute of Technology Roorkee, India in 2008. He is an Assistant Professor in the Department of Civil Engineering, Sardar Vallabhbhai Patel Institute of Technology, Vasad, India. His area of specialisation is Structural Engineeing.

A.K.Ahuja is a Professor in the Department of Civil Engineering, Indian Institute of Technology Roorkee, India He has more than 25 years of experience in teaching and research. His area of specialisation is Structural Engineering

Received October 2010
Accepted March 2011
Final acceptance in revised form May 2011